

# Burstiness and Memory in Complex Systems

Kwang-Il Goh<sup>1,2</sup> and Albert-László Barabási<sup>1</sup>

<sup>1</sup>Center for Complex Network Research and Department of Physics,  
225 Nieuwland Science Hall, University of Notre Dame, Notre Dame, IN 46556, USA  
<sup>2</sup>Department of Physics, Korea University, Seoul 136-713, Korea

(Dated: February 2, 2008)

The dynamics of a wide range of real systems, from email patterns to earthquakes, display a bursty, intermittent nature, characterized by short timeframes of intensive activity followed by long times of no or reduced activity. The understanding of the origin of such bursty patterns is hindered by the lack of tools to compare different systems using a common framework. We introduce two measures to distinguish the mechanisms responsible for the bursty nature of real signals, changes in the interevent times and memory. We find that while the burstiness of natural phenomena is rooted in both the interevent time distribution and memory, for human dynamics memory is weak, and the bursty character is due to changes in the interevent time distribution. Finally, we show that current models lack in their ability to reproduce the activity pattern observed in real systems, opening up new avenues for future work.

PACS numbers: 89.75.-k, 05.45.Tp

The dynamics of most complex systems is driven by the loosely coordinated activity of a large number of components, such as individuals in the society or molecules in the cell. While we witnessed much progress in the study of the networks behind these systems [1], advances towards understanding the system's dynamics has been slower. With increasing potential to monitor the time-resolved activity of most components of selected complex systems, such as time-resolved email [2, 3, 4], web browsing [5], and gene expression [6] patterns, we have the opportunity to ask an important question: is the dynamics of complex systems governed by generic organizing principles, or each system has its own distinct dynamical features? While it is difficult to offer a definite answer to this question, a common feature across many systems is increasingly documented: the burstiness of the system's activity patterns.

Bursts, vaguely corresponding to significantly enhanced activity levels over short periods of time followed by long periods of inactivity, have been observed in a wide range of systems, from email patterns [3] to earthquakes [7, 8] and gene expression [6]. Yet, often burstiness is more of a metaphor than a quantitative feature, and opinions about its origin diverge. In human dynamics, burstiness has been reduced to the fat-tailed nature of the response time distribution [3, 4], in contrast with earthquakes and weather patterns, where memory effects appear to play a key role [9, 10]. Once present, burstiness can affect the spreading of viruses [3] or resource allocation [11]. Also, deviations towards regular, "anti-bursty" behavior in heartbeat may indicate disease progression [12]. Given the diversity of systems in which it emerges, there is a need to place burstiness on a strong quantitative basis. Our goal in this paper is to make a first step in this direction, by developing measures that can help quantify the magnitude and potential origin of the bursty patterns seen in different real systems.

Let us consider a system whose components have a measurable activity pattern that can be mapped into a discrete signal, recording the moments when some events take place, like an email being sent, or a protein being translated. The activity pattern is random (Poisson process) if the probability of an event is time-independent. In this case the interevent time between two consecutive events ( $\tau$ ) follows an exponential distribution,  $P_P(\tau) \sim \exp(-\tau/\tau_0)$  (Fig. 1a). An apparently bursty (or anti-bursty) signal could emerge if  $P(\tau)$  is different from the exponential, such as the bursty pattern of Fig. 1b, or the more regular pattern of Fig. 1c. Yet, changes in the interevent time distribution is not the only way to generate a bursty signal. For example, the signals shown in Fig. 1d,e have exactly the same  $P(\tau)$  as in Fig. 1a, yet they have a more bursty or a more regular character. This is achieved by introducing memory: in Fig. 1d the short interevent times tend to follow short ones, resulting in a bursty look. In Fig. 1e the relative regularity is due to a memory effect acting in the opposite direction: short (long) interevent times tend to be followed by long (short) ones. Therefore, the apparent burstiness of a signal can be rooted in two, mechanistically quite different deviations from a Poisson process: changes in the interevent time distribution or memory. To distinguish these effects, we introduce the burstiness parameter  $\Delta$  and the memory parameter  $\mu$ , that quantify the relative contribution of each in real systems.

The *burstiness parameter*  $\Delta$  is defined as

$$\Delta \equiv \frac{\text{sgn}(\sigma_\tau - m_\tau)}{2} \int_0^\infty |P(\tau) - P_P(\tau)| d\tau , \quad (1)$$

where  $m_\tau$  and  $\sigma_\tau$  are the mean and the standard deviation of  $P(\tau)$  [13]. The meaning of  $\Delta$  is illustrated in Fig. 1f-h, where we compare  $P(\tau)$  for a bursty- (Fig. 1f) and an anti-bursty (Fig. 1g) signal with a Poisson interevent time distribution. A signal will appear bursty

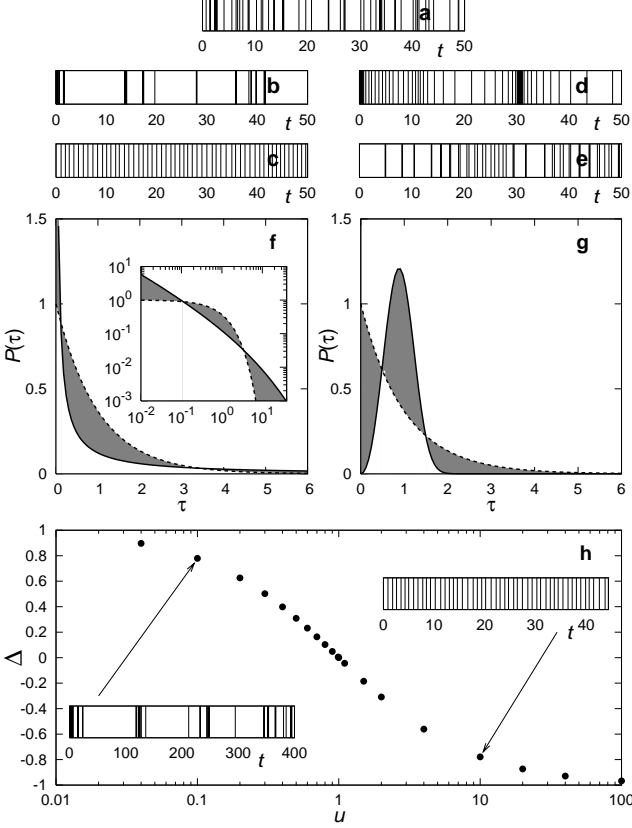


FIG. 1: (a) A signal generated by a Poisson process with a unit rate. (b,c) Bursty character through the interevent time distribution: A bursty signal (b) generated by the power-law interevent time distribution  $P(\tau) \sim \tau^{-1}$ , and an anti-bursty signal (c) generated by the Gaussian interevent time distribution with  $m = 1$  and  $\sigma = 0.1$ . A bursty signal can emerge through memory as well. For example, the bursty signal shown in (d) is obtained by shuffling the Poisson signal of (a) to increase the memory effect. A more regular looking signal, with negative memory, is obtained by the same shuffling procedure (e). Note that signals in (a), (d) and (e) have identical interevent time distribution. (f) An interevent time distribution (solid line) will appear bursty ( $\Delta > 0$ ) if it has a higher frequency of long or short interevent times than predicted for a Poisson process (dotted line). Inset shows the same curves in log-log scale. (g) The signal will appear to be regular (anti-bursty,  $\Delta < 0$ ) if  $P(\tau)$  is higher in the average interevent time region than a Poisson process. The burstiness parameter  $\Delta$  is half of the shaded area between the corresponding interevent time distribution (solid) and the reference distribution (dotted). (h) The stretched exponential distribution interpolates between a highly bursty ( $\Delta = 1$ ), a Poisson ( $\Delta = 0$ ), and a regular ( $\Delta = -1$ ) signal. The figure shows  $\Delta$  as a function of the parameter  $u$ .

if the frequency of the short and long interevent times is higher than in a random signal (Fig. 1f), resulting in many short intervals separated by longer periods of inactivity. Therefore, there are fewer interevent times of average length than in a Poisson process. A signal displays anti-bursty character, however, if the fre-

quency of the interevent times is enhanced near the average and depleted in the short and long interevent time region (Fig. 1g).  $\Delta$  is bounded in the range  $(-1, 1)$ , and its magnitude correlates with the signal's burstiness:  $\Delta = 1$  is the most bursty signal,  $\Delta = 0$  is completely neutral (Poisson), and  $\Delta = -1$  corresponds to a completely regular (periodic) signal. For example, in Fig. 1h we show  $\Delta$  for the stretched exponential distribution,  $P_{SE}(\tau) = u(\tau/\tau_0)^{u-1} \exp[-(\tau/\tau_0)^u]/\tau_0$ , often used to approximate the interevent time distributions of complex systems [14]. The smaller the  $u$  is, the burstier is the signal, and for  $u \rightarrow 0$ ,  $P_{SE}(\tau)$  follows a power law with the exponent  $-1$ , for which  $\Delta = 1$ . For  $u = 1$ ,  $P_{SE}(\tau)$  is simply the exponential distribution with  $\Delta = 0$ . Finally, for  $u > 1$ , the larger  $u$  is, the more regular is the signal, and for  $u \rightarrow \infty$ ,  $P(\tau)$  converges to a Dirac delta function with  $\Delta = -1$ .

Most complex systems display a remarkable heterogeneity: some components may be very active, and others much less so. For example, some users may send dozens of emails during a day, while others only one or two. To combine the activity levels of so different components, we can group the signals based on their average activity level, and measure  $P(\tau)$  only for components with similar activity level. As the insets in Fig. 2 show, the obtained curves are systematically shifted. If we plot, however,  $\tau_0 P(\tau)$  as a function of  $\tau/\tau_0$ , where  $\tau_0$  being the average interevent time, the data collapse into a single curve  $\mathcal{F}(x)$  (Fig. 2), indicating that the interevent time distribution follows  $P(\tau) = (1/\tau_0)\mathcal{F}(\tau/\tau_0)$ , where  $\mathcal{F}(x)$  is independent of the average activity level of the component, and represents an universal characteristic of the particular system [8, 15]. This raises an important question: will  $\Delta$  depend on  $\tau_0$ ? The burstiness parameter  $\Delta$  is invariant under the time rescaling as  $\tilde{\tau} \equiv \tau/\tau_0$  and  $\tilde{P}(\tilde{\tau}) \equiv \tau_0 P(\tau)$  with a constant  $\tau_0$ , since  $\tilde{\Delta} \equiv \int_0^\infty |\tilde{P}(\tilde{\tau}) - \tilde{P}_0(\tilde{\tau})| d\tilde{\tau} = \int_0^\infty |\tau_0 P(\tau) - \tau_0 P_0(\tau)| d(\tau/\tau_0) = \int_0^\infty |P(\tau) - P_0(\tau)| d\tau \equiv \Delta$ , i.e., it characterizes the universal function  $\mathcal{F}(x)$ . Such invariance of  $\Delta$  enables us to assign to each system a single burstiness parameter, despite the different activity level of its components.

The *memory coefficient*  $\mu$  of a signal is defined as the correlation coefficient of all consecutive interevent time values in the signal over a population. That is, given all pairs of consecutive interevent times  $(\tau_{k,i}, \tau_{k,i+1})$  for all components  $\{k = 1, \dots, N\}$ ,

$$\mu \equiv \frac{1}{N} \sum_{k=1}^N \sum_{i=1}^{n_k-1} \frac{(\tau_i - m_{k1})(\tau_{i+1} - m_{k2})}{\sigma_{k1}\sigma_{k2}}, \quad (2)$$

where  $N$  is the number of components in the system,  $n_k$  is the number of events recorded for component  $k$ , and  $m_{k1}$  ( $m_{k2}$ ) and  $\sigma_{k1}$  ( $\sigma_{k2}$ ) are the mean and standard deviation of  $\tau_{k,i}$ 's ( $\tau_{k,i+1}$ 's), respectively. The memory coefficient is positive when a short (long) interevent time tends to be followed by a short (long) one, and it is neg-

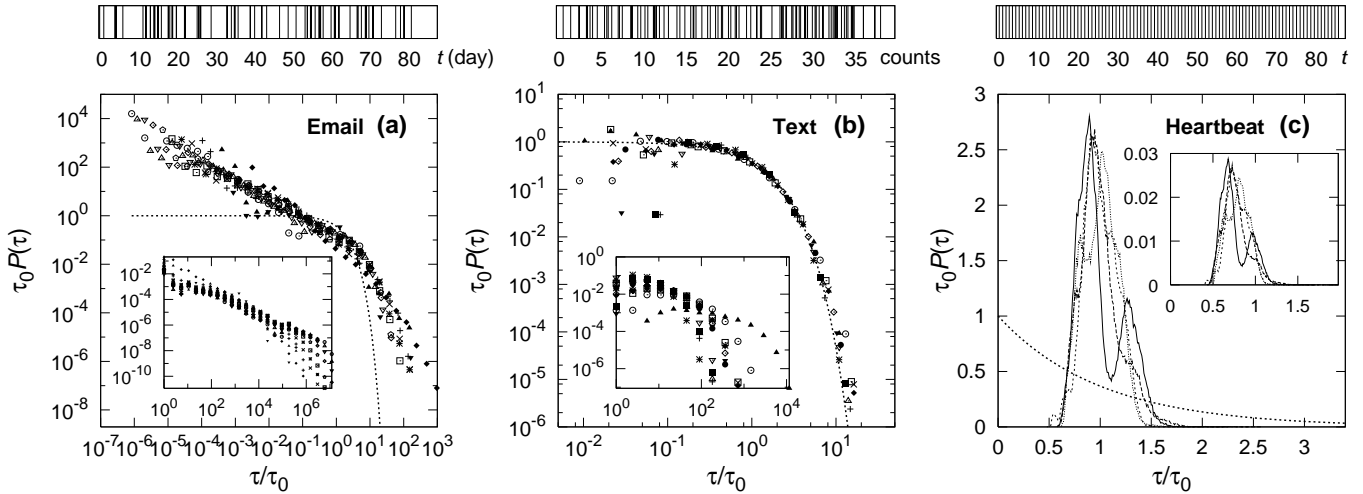


FIG. 2: Interevent time distributions  $P(\tau)$  for some real signals. (a)  $P(\tau)$  for e-mail activity of individuals from a University [2].  $\tau$  corresponds to the time interval between two emails sent by the same user. (b) Interevent time distribution for the occurrence of letter in the text of C. Dickens' *David Copperfield* [16]. (c) Interevent time distribution of cardiac rhythm of individuals [21]. Each event corresponds to the beat in the heartbeat signal. In each panel, we also show for reference the exponential interevent time distribution (dotted). Unscaled interevent time distribution is shown in the inset for each dataset.

ative when a short (long) interevent time is likely to be followed by a long (short) one. The measurements indicate that  $\mu$  is independent of  $\tau_0$ .

*Mapping complex systems on the  $(\mu, \Delta)$  space*— Given that the burstiness of a signal can have two qualitatively different origins, the best way to characterize a real system is to identify its  $\mu$  and  $\Delta$  parameters, placing them in a  $(\mu, \Delta)$  phase diagram (Fig. 3). As a first example, we measured the spacing between the consecutive occurrence of the same letter in texts of different kind, era, and language [16]. For these signals, we find  $\Delta \approx 0$ , *i.e.*, the interevent time distribution follows closely an exponential (Fig. 2b) and  $\mu \approx 0.01$ , indicating the lack of memory. Thus this signal is best described by a Poisson process, at the origin of the phase diagram (Fig. 3). In contrast, natural phenomena, like earthquakes [17] and weather patterns [18] are in the vicinity of the diagonal, indicating that  $P(\tau)$  and memory equally contribute to their bursty character. The situation is quite different, however, for human activity, ranging from email and phone communication to web browsing and library visitation patterns [2, 4, 5, 20]. For these we find a high  $\Delta$  and small or negligible  $\mu$ , indicating that while these systems display significant burstiness rooted in  $P(\tau)$ , memory plays a small role in their temporal inhomogeneity. This lack of memory is quite unexpected, as it suggests the lack of predictability in these systems in contrast with natural phenomena, where strong memory effects could lead to predictive tools. Finally for cardiac rhythms describing the time between two consecutive heartbeats (Fig. 2c) [21], we find  $\Delta_{\text{cardiac, healthy}} = -0.73(4)$  for healthy individuals and  $\Delta_{\text{cardiac, CHF}} = -0.82(6)$  for patients with congestive heart failure (CHF), both signals being highly

regular. Thus the  $\Delta$  parameter captures the fact that cardiac rhythm is more regular with CHF than in the healthy condition [12]. Furthermore, we find  $\mu \approx 0.97$ , indicating that memory also plays a very important role in the signal's regularity.

The discriminative nature of the  $(\mu, \Delta)$  phase diagram is illustrated by the non-random placement of the different systems in the plane: human activity patterns cluster together in the high  $\Delta$ , low  $\mu$  region, natural phenomena near the diagonal, heartbeats in the high  $\mu$ , negative  $\Delta$  region and texts near  $\Delta = \mu = 0$ , underlying the existence of distinct classes of dynamical mechanisms driving the temporal activity in these systems.

Following the clustering of the empirical measurements in the phase diagram, a natural question emerges: to what degree can current models reproduce the observed quantitative features of bursty processes? Queueing models, proposed to capture human activity patterns, are designed to capture the waiting times of the tasks, rather than interevent times [3, 4, 22]. Therefore, placing them on the phase diagram is not meaningful. A bursty signal can be generated by 2-state model [23], switching with probability  $p$  its internal state between Poisson processes with two different rates  $\lambda_0 < \lambda_1$ .  $\Delta$  for the model is independent of  $p$  in the long time limit as long as  $p > 0$ , and takes its value in the range  $0 < \Delta < 0.5$ , approaching 0 when  $\lambda_0 \approx \lambda_1$  and 0.5 as  $\lambda_1 \rightarrow \infty$  and  $\lambda_0 \rightarrow 0$ . The memory coefficient of the model follows  $\mu = A(0.5 - p)$ , where  $A$  is a positive constant dependent on  $\lambda_0$  and  $\lambda_1$  so that  $-1/3 < \mu < 1/3$ . The region in the  $(\mu, \Delta)$  space occupied by the model is shown in the light grey area in Fig. 3a, suggesting that by changing its parameters the model could account for all observed behaviors. Yet,

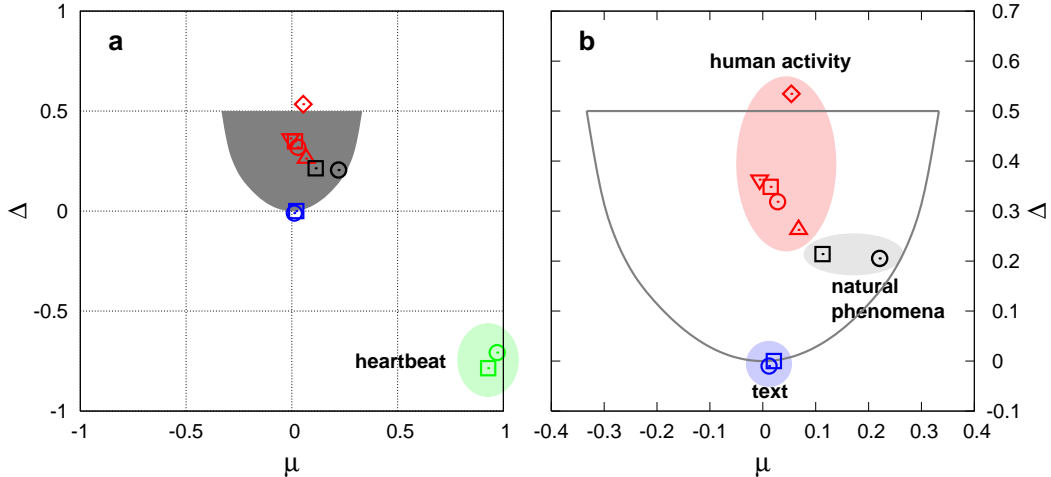


FIG. 3: (Color) (a) The  $(\mu, \Delta)$  phase diagram. Human behaviors (red) are captured by activity patterns pertaining to email ( $\square$ ) [2], library loans ( $\circ$ ) [4], and printing ( $\diamond$ ) [19] of individuals in Universities, call center record at an anonymous bank ( $\triangle$ ) [20], and phone initiation record from a mobile phone company ( $\nabla$ ). Data for natural phenomena (black) are earthquake records in Japan ( $\circ$ ) [17] and daily precipitation record in New Mexico, USA ( $\square$ ) [18]. Data for human texts (blue) [16] are the English text of *David Copperfield* ( $\circ$ ) and the Hungarian text of *Isten Rabjai* by Gárdonyi Géza ( $\square$ ). Data for physiological behaviors (green) are the normal sinus rhythm ( $\circ$ ) and the cardiac rhythm with CHF ( $\square$ ) of human subjects [21]. Grey area is the region occupied by the 2-state model [23]. (b) Close-up of the most populated region.

the agreement is misleading: for example, for human activities  $P(\tau)$  is fat-tailed, which is not the case for the model. This indicates that  $\Delta$  and  $\mu$  offer only a first order approximation for the origin of the burstiness, and for a detailed comparison between models and real systems we need to inspect other measures as well, such as the functional form of  $P(\tau)$ . It also indicates the lack of proper modeling tools to capture the detailed mechanisms responsible for the bursty interevent time distributions seen in real systems, opening up possibilities for future work.

We would like to thank S. Havlin and A. Vázquez for helpful discussions. This work is supported by the S. McDonnell Foundation and the National Science Foundation under Grant No. CNS-0540348 and ITR DMR-0426737.

- [1] S. N. Dorogovtsev and J. F. F. Mendes, *Evolution of Networks* (Oxford University Press, Oxford, 2002); M. E. J. Newman, SIAM Rev. **45**, 167 (2003); R. Pastor-Satorras and A. Vespignani, *Structure and evolution of the Internet* (Cambridge University Press, Cambridge, 2003); S. Boccaletti, *et al.*, Phys. Rep. **424**, 175 (2006); M. E. J. Newman, D. J. Watts, and A.-L. Barabási (eds.), *Structure and Dynamics of Complex Networks* (Princeton University Press, Princeton, 2006).
- [2] J. P. Eckmann, E. Moses, and D. Sergi, Proc. Natl. Acad. Sci. U.S.A. **101**, 14333 (2004).
- [3] A.-L. Barabási, Nature (London) **207**, 435 (2005); A. Vázquez, Phys. Rev. Lett. **95**, 248701 (2005).
- [4] A. Vázquez, *et al.*, Phys. Rev. E **73**, 036127 (2006).
- [5] Z. Dezső, *et al.*, Phys. Rev. E **73**, 066132 (2006).
- [6] I. Golding, *et al.*, Cell **123**, 1025 (2005); J. R. Chubb, *et al.*, Curr. Biol. **16**, 1018 (2006).
- [7] P. Bak, *et al.*, Phys. Rev. Lett. **88**, 178501 (2002).
- [8] A. Corral, Phys. Rev. E **68**, 035102(R) (2003).
- [9] A. Bunde, *et al.*, Phys. Rev. Lett. **94**, 048701 (2005).
- [10] V. N. Livina, S. Havlin, and A. Bunde, Phys. Rev. Lett. **95**, 208501 (2005).
- [11] W. E. Leland, *et al.*, IEEE/ACM Trans. Networking **2**, 1 (1994).
- [12] S. Thurner, M. C. Feurstein, and M. C. Teich, Phys. Rev. Lett. **80**, 1544 (1998).
- [13] As an alternative,  $\sigma_\tau/m_\tau$  can also be used instead of  $\Delta$  to measure burstiness [A. Vázquez, private communications].
- [14] J. Laherrère and D. Sornette, Eur. Phys. J. B **2**, 525 (1998).
- [15] A. Saichev and D. Sornette, Phys. Rev. Lett. **97**, 078501 (2006).
- [16] Project Gutenberg, <http://gutenberg.org>.
- [17] Japan University Network Earthquake Catalog, <http://wwwweic.eri.u-tokyo.ac.jp/CATALOG/junec/>.
- [18] National Resources Conservation Service, <http://www.nm.nrcs.usda.gov/snow/data/historic.htm>.
- [19] U. Harder and M. Paczuski, Physica A **361**, 329 (2006).
- [20] I. Guedj and A. Mandelbaum, <http://iew3.technion.ac.il/serveng/callcenterdata/>.
- [21] PhysioBank, <http://www.physionet.org/physiobank/>.
- [22] J. G. Oliveira and A.-L. Barabási, Nature (London) **437**, 1251 (2005).
- [23] J. Kleinberg, Proc. ACM SIGKDD '02, pp. 91 (2002).